Journal of Visualized Experiments

Fabrication of 3D Cardiac Microtissue Arrays Using Human iPSC-Derived Cardiomyocytes, Cardiac Fibroblasts, and Endothelial Cells

--Manuscript Draft--

Article Type:	Invited Methods Article - JoVE Produced Video
Manuscript Number:	JoVE61879R2
Full Title:	Fabrication of 3D Cardiac Microtissue Arrays Using Human iPSC-Derived Cardiomyocytes, Cardiac Fibroblasts, and Endothelial Cells
Corresponding Author:	Joseph Wu, MD, PhD Stanford University School of Medicine Stanford, CA UNITED STATES
Corresponding Author's Institution:	Stanford University School of Medicine
Corresponding Author E-Mail:	joewu@stanford.edu
Order of Authors:	Dilip Thomas
	Hyeonyu Kim
	Nicole Lopez
	Joseph Wu, MD, PhD
Additional Information:	
Question	Response
Please indicate whether this article will be Standard Access or Open Access.	Standard Access (US$2,400)
Please indicate the **city, state/province, and country** where this article will be **filmed**. Please do not use abbreviations.	Stanford, California, USA
Please confirm that you have read and agree to the terms and conditions of the author license agreement that applies below:	I agree to the Author License Agreement
Please specify the section of the submitted manuscript.	Bioengineering
Please provide any comments to the journal here.	

1   **TITLE:**
2   Fabrication of 3D Cardiac Microtissue Arrays Using Human iPSC-Derived Cardiomyocytes, Cardiac
3   Fibroblasts, and Endothelial Cells
4
5   **AUTHORS AND AFFILIATIONS:**
6   Dilip Thomas[1], Hyeonyu Kim[1], Nicole Lopez[1], Joseph C. Wu[1,2,3]
7
8   [1]Stanford Cardiovascular Institute, Stanford, CA 94305, USA
9   [2]Department of Medicine, Division of Cardiovascular Medicine, Stanford, CA 94305, USA
10 [3]Department of Radiology, Stanford, CA 94305, USA
11
12 Email addresses of co-authors:
13 Dilip Thomas   (dilipt@stanford.edu)
14 Hyeonyu Kim   (hyeonyu@stanford.edu)
15 Nicole Lopez   (nicolelz@stanford.edu)
16 Joseph C. Wu (joewu@stanford.edu)
17
18 Corresponding Author:
19 Joseph C. Wu (joewu@stanford.edu)
20
21 **KEYWORDS:**
22 iPSC; cardiomyocytes; endothelial cells; fibroblasts; microtissues; self-assembly
23
24 **SUMMARY:**
25 Here, we describe an easy-to-use methodology to generate 3D self-assembled cardiac
26 microtissue arrays composed of pre-differentiated human-induced pluripotent stem cell-derived
27 cardiomyocytes, cardiac fibroblasts, and endothelial cells. This user-friendly and low cell
28 requiring technique to generate cardiac microtissues can be implemented for disease modeling
29 and early stages of drug development.
30

31 **ABSTRACT:**
32 Generation of human cardiomyocytes (CMs), cardiac fibroblasts (CFs), and endothelial cells (ECs)
33 from induced pluripotent stem cells (iPSCs) has provided a unique opportunity to study the
34 complex interplay among different cardiovascular cell types that drives tissue development and
35 disease. In the area of cardiac tissue models, several sophisticated three-dimensional (3D)
36 approaches use induced pluripotent stem cell-derived cardiomyocytes (iPSC-CMs) to mimic
37 physiological relevance and native tissue environment with a combination of extracellular
38 matrices and crosslinkers. However, these systems are complex to fabricate without
39 microfabrication expertise and require several weeks to self-assemble. Most importantly, many
40 of these systems cannot easily generate vascular cells and cardiac fibroblasts that make up over
41 60% of the nonmyocytes in the human heart. Here we describe the derivation of all three cardiac
42 cell types to fabricate cardiac microtissues. This facile replica molding technique allows cardiac
43 microtissue culture in standard multi-well cell culture plates for several weeks. The platform
44 allows user-defined control over microtissue sizes based on initial seeding density and requires

45 less than 3 days for self-assembly to achieve observable cardiac microtissue contractions.
46 Furthermore, the cardiac microtissues can be easily digested while maintaining high cell viability
47 for single-cell interrogation with the use of flow cytometry and single-cell RNA sequencing
48 (scRNA-seq). We envision that this *in vitro* model of cardiac microtissues will help accelerate
49 validation studies in drug discovery and disease modeling.
50
51 **INTRODUCTION:**
52 Drug discovery and disease modeling in the field of cardiovascular research face several
53 challenges due to a lack of clinically relevant samples and inadequate translational tools[1]. Highly
54 complex pre-clinical models or oversimplified *in vitro* single-cell models do not exhibit
55 pathophysiological conditions in a reproducible manner. Therefore, several miniaturized tissue-
56 engineered platforms have evolved to help bridge the gap, with the goal of achieving a balance
57 between ease of application in a high-throughput manner and faithful recapitulation of tissue
58 function[2,3]. With the advent of induced pluripotent stem cell (iPSC) technology, tissue
59 engineering tools can be applied to patient-specific cells with or without underlying
60 cardiovascular disease state to answer research questions[4–6]. Such tissue engineered models
61 with cellular composition similar to the heart tissue could be utilized in drug development efforts
62 to test for cardiotoxicity and dysfunction induced by pathological changes in behavior of one or
63 multiple cell types.
64
65 Self-assembled microtissues or organoids derived from human iPSCs are three-dimensional (3D)
66 structures that are miniature tissue-like assemblies exhibiting functional similarities to their *in*
67 *vivo* counterparts. There are several different approaches that allow formation of organoids *in*
68 *situ* via directed differentiation of iPSCs or through formation of embryoid bodies[4]. The resulting
69 organoids are an indispensable tool to study morphogenetic processes that drive organogenesis.
70 However, the presence of a variety of cell populations and differences in self-organization can
71 lead to variability in outcomes between different organoids[5]. Alternatively, pre-differentiated
72 cells that are self-assembled into microtissues with tissue-specific cell types to study local cell-
73 cell interactions are excellent models, where it is feasible to isolate the self-assembled
74 components. Particularly in human cardiac research, development of 3D cardiac microtissues
75 with multicellular components has proven to be challenging when cells are derived from different
76 patient lines or commercial sources.
77
78 To improve our mechanistic understanding of cell behaviors in a physiologically relevant,
79 personalized, *in vitro* model, ideally all component cell types should be derived from the same
80 patient line. In the context of a human heart, a truly representative cardiac *in vitro* model would
81 capture the crosstalk among predominant cell types, namely, cardiomyocytes (CMs), endothelial
82 cells (ECs), and cardiac fibroblasts (CFs)[6,7]. The faithful recapitulation of a myocardium not only
83 requires biophysical stretch and electrophysiological stimulation, but also cell-cell signaling that
84 arise from supporting cell types such as ECs and CFs[8]. CFs are involved in the synthesis of
85 extracellular matrix and maintaining tissue structure; and in a pathological state, CFs can induce
86 fibrosis and alter electrical conduction in the CMs[9]. Similarly, ECs can regulate contractile
87 properties of CMs through paracrine signaling and supplying vital metabolic demands[10]. Hence,
88 there is a need for human cardiac microtissues composed of all three major cell types to allow

89   physiologically relevant high-throughput experiments to be conducted.
90
91   Here, we describe a bottom-up approach in fabrication of cardiac microtissues by derivation of
92   human iPSC-derived cardiomyocytes (iPSC-CMs), iPSC-derived endothelial cells (iPSC-ECs), and
93   iPSC-derived cardiac fibroblasts (iPSC-CFs) and their 3D culture in uniform cardiac microtissue
94   arrays. This facile method of generating spontaneously beating cardiac microtissues can be
95   utilized for disease modeling and rapid testing of drugs for functional and mechanistic
96   understanding of heart physiology. Furthermore, such multicellular cardiac microtissue platforms
97   could be exploited with genome editing techniques to emulate cardiac disease progression over
98   time under chronic or acute culture conditions.
99
100 **PROTOCOL:**
101
102 **1.   Medium, reagent, culture plate preparation**
103
104 1.1   Cell wash solution for cell culture: Use 1x phosphate buffered saline (PBS) or Hanks
105 balanced salt solution (HBSS) without calcium or magnesium.
106
107 1.2   Cardiomyocyte differentiation media
108
109 1.2.1   Prepare differentiation Medium #1 by adding 10 mL supplement (50x B27 plus insulin) to
110 500 mL cardiomyocyte basal medium (RPMI 1640).
111
112 1.2.2   Prepare differentiation Medium #2 by adding 10 mL supplement (50x B27 minus insulin)
113 to 500 mL cardiomyocyte basal medium (RPMI 1640).
114
115 1.2.3   Prepare purification Medium #3 by adding supplement (50x B27 plus insulin) to 500 mL
116 cardiomyocyte basal medium (RPMI 1640) minus glucose.
117
118 1.3. Magnetic-activated cell sorting (MACS) reagents
119
120 1.3.1. Prepare endothelial growth medium (EGM) with commercially available endothelial cell
121 growth medium supplement kit.
122
123 1.3.2. Prepare cell separation sorting buffer solution by diluting bovine serum albumin (BSA)
124 stock solution to 1:20 with rinsing solution.
125
126 1.4.   Cardiac fibroblast differentiation medium: Prepare cardiac fibroblast differentiation
127 medium with fibroblast basal medium (DMEM—high glucose) and Serum-Free Fibroblast Life
128 Factors kit.
129
130 1.5.   Cardiac microtissue fabrication and maintenance medium: Prepare filtered medium with
131 cardiomyocyte basal medium (RPMI 1640) with supplement (50x B27 plus insulin) and EGM in
132 70/30 v/v% ratio.

133

134   1.6.   Small molecule and growth factor stock solutions

135

136   1.6.1. For differentiation of all three cell types, prepare 200 µL aliquots of GSK3-beta inhibitor
137   **CHIR   99021**   (6-[[2-[[4-(2,4-Dichlorophenyl)-5-(5-methyl-1H-imidazol-2-yl)-2-
138   pyrimidinyl]amino]ethyl]amino]-3-pyridinecarbonitrile);   Wnt   inhibitor   **IWR-1-endo**   (4-
139   (1,3,3a,4,7,7a-Hexahydro-1,3-dioxo-4,7-methano-2H-isoindol-2-yl)-N-8-quinolinyl-Benzamide;
140   and transforming growth factor beta (TGF-β) inhibitor **SB431542** (4-[4-(1,3-Benzodioxol-5-yl)-5-
141   (2-pyridinyl)-1H-imidazol-2-yl]benzamid) at 10 mM concentration in dimethyl sulfoxide (DMSO).

142

143   1.6.2. For human iPSC-EC differentiation, prepare 100 µL aliquots of basic fibroblast growth
144   factor (bFGF) (20 µg/mL), vascular endothelial growth factor 165 (VEGF$_{165}$; 50 µg/mL), and bone
145   morphogenetic protein 4 (BMP4; 20 µg/mL) in 0.1% (w/v) BSA in ultrapure distilled water. Store
146   the aliquots at -20 °C; for long-term storage, aliquots can be stored at -80 °C for up to 1 year.

147

148   1.7.   Pre-coating plates for maintenance of iPSC-CMs, iPSC-ECs, and iPSC-CFs.

149

150   1.7.1. Prepare basement membrane matrix medium coated 6-well plates for iPSC-CM re-plating
151   by diluting Growth Factor Reduced (GFR) basement membrane matrix medium in DMEM/F12 in
152   a 1:200 ratio. Add 2 mL of diluted basement membrane matrix medium to each well of the 6-well
153   plate and leave it to set for at least 2 to 4 h.

154

155   1.7.2. Pre-coat 6-well plate or 10 cm dish with gelatin. Liquefy 2% gelatin solution in a water
156   bath at 37 °C and prepare filtered 0.2% (vol/vol) gelatin in PBS in an appropriate volume as
157   needed. Coat the culture plate with 10 mL of 0.2% gelatin for at least 30 min at 37 °C prior to use.

158

159   NOTE: Gelatin plates can be used for both iPSC-CFs and iPSC-ECs after MACS.

160

161   1.8.   Fabrication of microtissue molds: Prepare 2% low melting agarose solution in PBS in a dry
162   100 mL glass bottle. Sterilize the agarose at 121 °C, 15 psi for 20 min prior to use. Autoclave the
163   casting silicone micro-molds at 121 °C, 15 psi for 15 min.

164

165   1.9.   Solutions for digestion, immunostaining, and flow cytometry

166

167   1.9.1. For microtissue digestion, prepare an enzyme digestion buffer of Dispase I (1 U/mL) and
168   Liberase (0.3 U/mL) in PBS. Keep this solution on ice.

169

170   1.9.2. For both cell and microtissue fixation, use ice cold commercially available fixation reagent
171   containing 4.2% paraformaldehyde (PFA).

172

173   1.9.3. Prepare 0.25% Triton X-100 in PBS for permeabilization and 0.1% Tween-20 for washes.
174   The solution can be stored at room temperature.

175

176   1.9.4. For fluorescence-activated cell sorting (FACS) analyses, prepare FACS buffer [PBS or HBSS

177 with 2% fetal bovine serum (FBS)] and store at 4 °C.
178
179 1.9.5. For immunostaining, prepare 2% normal goat/donkey/rabbit serum in PBS. Choose the
180 serum species based on the host in which the antibodies were raised.
181
2.   Cardiac differentiation and purification

183
184 NOTE: All iPSCs should be maintained at ~75% to 80% confluency prior to cardiomyocyte
185 differentiation. iPSCs used for this protocol were derived from peripheral blood mononuclear
186 cells (PBMCs) using Sendai virus reprogramming performed at the Stanford Cardiovascular
187 Institute (SCVI) Biobank.
188
189 2.1.   Prior to differentiation, culture iPSC colonies up to passage (P20).
190
191 2.2.   Remove the iPSC culture medium from the 6-well plate and wash the cells once with 2 mL
192 PBS.
193
194 2.3.   On day 0, begin mesendoderm induction by adding 2 mL of differentiation Medium #1
195 with CHIR (6 μM final) in each well. The final concentration may vary between 6 to 9 μM for
196 different iPSC lines. Hence, it is recommended to test different CHIR concentrations on a 6-well
197 plate to identify optimal cardiac mesoderm induction.
198
199 2.4.   On day 2, recover the cells by replacing with fresh 2 mL Medium #1 in each well.
200
201 2.5.   On day 3, replace medium in each well with 2 mL differentiation Medium #1 with Wnt
202 inhibitor IWR-1-endo (5 μM) to induce cardiac-lineage specification.
203
204 2.6.   On day 5, recover the cells by replacing medium with fresh 2 mL Medium #1 in each well.
205
206 2.7.   On day 7, replace medium with 2 mL Medium #2 in each well. Spontaneous beating of
207 cardiomyocytes may be observed as early as day 8–9. For some lines, beating cells may appear
208 as late as day 11.
209
210 2.8.   For purification of the differentiation culture, replace with 2 mL minus glucose Medium
211 #3 in each well on day 10.
212
213 2.9.   On day 13, recover the cells by changing the medium with 2 mL plus glucose Medium #2
214 in each well.
215
216 2.10.   On day 16, perform second round of purification with 2 mL of Medium #3 in each well.
217
218 2.11.   Recover the cells on day 19 with 2 mL plus glucose Medium #2.
219
220 2.12.   On day 20, wash the wells once with 1 mL PBS and dissociate the cells using 1 mL 10x

221 Trypsin for 6 min at 37 °C. After incubation, the cells are lifted off the well surface into single cells
222 for less than 15 s and added to 15 mL conical tube with equal volume of Medium #2 to neutralize
223 the enzyme. Centrifuge the cell suspension for 3 min at 270 x g.

225 2.13.   Resuspend the cell pellet in 3 mL Medium #3. Count the cells and add appropriate volume
226 of Medium #3 to plate a total of ~3 million cells in each well of a new basement membrane matrix
227 medium coated 6-well plate. On the second day after re-plating, replace the medium with fresh
228 2 mL Medium #2, and replenish with 2 mL Medium #2 every other day until trypsinization of
229 cardiomyocytes for freezing or experiments.

231 **3.   Endothelial cell differentiation and MACS sorting**

233 3.1.   At 75% to 80% iPSC confluency, wash the plate with PBS, 2 mL per well.

235 3.2.   Begin differentiation at day 0 by replacing with 2 mL of differentiation Medium #1 with 6
236 µM CHIR.

238 3.3.   On day 2, replace the medium with 2 mL of differentiation Medium #1 with 2 µM CHIR.

240 3.4.   On day 4, replace the medium with 2 mL of EGM supplemented with 20 ng bFGF-2, 50 ng
241 $VEGF_{165}$, and 20 ng BMP4.

243 3.5.   Change the medium with 2 mL of EGM supplemented with growth factors every 2 days
244 from day 6 to day 10. Addition of TGFβ inhibitor (SB431542) at 8 µM concentration is optional to
245 promote endothelial expansion and suppress differentiation of other mesenchymal origin cell
246 types.

248 3.6.   On day 12, begin steps for MACS sorting by rinsing each well with 1 mL of PBS followed
249 by cell dissociation using 1 mL of 10x Trypsin in each well of a 6-well plate for 8 min at 37 °C.

251 3.7.   Prepare an equal volume of EGM medium in a 50 mL conical tube to neutralize the
252 dissociation enzyme. Place a 40 µm cell strainer on the 50 mL conical tube and pass the
253 dissociated cell suspension through the strainer. Change the filter for every 2 to 3 dissociated
254 wells.

256 3.8.   Enumerate the total viable cells using 0.4% Trypan blue using a hemocytometer or an
257 automated cell counter.

259 3.9.   Pellet the cell suspension at 300 x g for 5 min in a pre-cooled centrifuge set at 4 °C.

261 3.10.   Discard the supernatant and resuspend the cell pellet in appropriate volume of sorting
262 buffer based on the total count in step 3.8.

264 NOTE: Add 80 µL of sorting buffer per 10^7 total cells.

265

266   3.11.   For magnetic bead labeling, add 20 µL of FcR Blocking reagent per 10^7 cells and incubate
267   for 5 min.

268

269   3.12.   Add 20 µL of CD144 or CD31 Microbeads per 10^7 cells and mix well. Incubate the cell
270   suspension in dark at 4 °C for 15 min.

271

272   3.13.   Add 20 mL of sorting buffer to wash the labeled cells and pellet the cells 300 x g for 5 min
273   in a pre-cooled centrifuge set at 4 °C.

274

275   3.14.   Resuspend the cell pellet in 3 mL of sorting buffer and leave it on ice.

276

277   3.15.   Prepare a magnetic separation column by placing the column in the separator notch.

278

279   3.16.   Equilibrate the column by rinsing with 3 mL of sorting buffer and collect the flow through
280   in a waste conical tube.

281

282   3.17.   Once the rinsing buffer flows through, resuspend the cell suspension thoroughly to break
283   any clumps and apply the cell suspension onto the column.

284

285   3.18.   After the cell suspension has flowed through, wash the column with 3 mL of sorting buffer
286   three times to remove any unlabeled cells.

287

288   3.19.   Remove the column from the separator and place it in a 15 mL conical tube for
289    $CD144^+/CD31^+$ cell elution.

290

291   3.20.   Add 5 mL of sorting buffer onto the column and immediately flush the magnetically
292   labeled cells with the plunger.

293

294   3.21.   Determine the viable cell number using 0.4% Trypan blue using a hemocytometer or an
295   automated cell counter.

296

297   3.22.   Centrifuge the cell suspension in a pre-cooled centrifuge at 300 x g for 3 min.

298

299   3.23.   Resuspend the cell pellet in appropriate volume of EGM with 5–8 µM of TGFβ inhibitor
300   (SB431542) based on the total count in step 3.21.

301

302   3.24.   Plate this passage 0 (P0) cells at an appropriate cell density (4 x 10^4 cells/cm^2) on a pre-
303   coated 0.2% gelatin plate.

304

305   3.25.   For P0 and P1, continue to replenish the medium with fresh EGM every 2 days with TGFβ
306   inhibitor. From P2, cells can be cultured in endothelial growth medium without TGFβ inhibitor.

307

308   **4.   Cardiac fibroblast differentiation**

309

4.1.　　Allow iPSCs to become 90% to 95% confluent; wash each well with 1 mL PBS.

4.2.　　Begin differentiation at day 0 by adding 2 mL of differentiation Medium #1 with 11 μM CHIR. For sensitive iPSC lines, the concentration may vary between 9–10 μM.

4.3.　　On day 1, observe the plate. It is normal to observe significant cell death with ~30% to 40% cells adhered to the plate.

4.4.　　On day 3, add 2 mL of differentiation Medium #1 with 5 μM IWR-1-endo to promote expansion of cardiac progenitors.

4.5.　　On day 4, replace the medium with 2 mL of cardiac fibroblast differentiation medium. Replace with fresh medium every 2 days till day 16.

4.6.　　On day 18, detach the cells using 1 mL of 10x Trypsin in each well of a 6-well plate for 10 min at 37 °C.

4.7.　　Disrupt the cell layer thoroughly and pass the cell suspension through a 70 μM cell strainer in a 50 mL conical tube containing equal volume of DMEM/F12 medium supplemented with 5% FBS.

4.8.　　Determine the viable cell number using 0.4% Trypan blue using a hemocytometer or an automated cell counter.

4.9.　　Centrifuge the cell suspension at 300 x g for 5 min to obtain a pellet.

4.10.　For the first re-plating, resuspend the cell pellet in an appropriate volume of differentiation medium and plate at a cell density (6 x 10^4 cells/cm^2) on a 0.2% gelatin coated plate until 90% confluency.

4.11.　Split the plate and maintain the cardiac fibroblasts in regular DMEM/F12 with 10% serum on gelatin coated plates.

5.　　　Casting of cardiac microtissue molds and cell seeding

5.1.　　Melt the agarose in a microwave in a 100 mL glass bottle until boiling. Spray the agarose bottle and place it in the biosafety cabinet. Allow the agarose to cool down for ~3 min.

5.2.　　Pipette 700 μL of molten agarose in a silicone micro-mold of 9 x 9 array. Avoid generating bubbles while pipetting.

5.3.　　Carefully place the mold on a pre-cooled ice block to accelerate agarose gelation.

5.4.   Ensure that once the agarose is gelled, it becomes translucent. Carefully bend around the edges of the micro-mold to loosen the agarose replica. Then, gently peel the replica from all sides to detach the agarose replica from the silicone micro-mold.

5.5.   Transfer the agarose microtissue tray containing 81 circular recesses (800 μm diameter; 800 μm depth) into a sterile 12-well plate.

5.6.   Add 2 mL of PBS to the agarose microtissue tray and inspect under the microscope for any trapped bubbles or irregular shaped wells.

5.7.   Submerge the agarose tray in 2 mL 70% ethanol overnight, followed by UV treatment in the biosafety cabinet for 1 h.

5.8.   Prior to use, remove the 70% ethanol and wash twice with distilled water and a final wash with 2 mL PBS.

5.9.   Trypsinize, neutralize, and count iPSC-CMs, iPSC-ECs, and iPSC-CFs and place the cell suspensions on ice.

5.10.   Remove the PBS from the well and the cell seeding chamber carefully without touching the recesses.

5.11.   In a new tube, mix iPSC-CMs, iPSC-ECs, and iPSC-CFs in 7:2:1 ratio, respectively, to achieve a final cell density of 10^6 cells/mL. Higher cell densities will result in larger microtissues.

NOTE: Do not exceed 2 x 10^6 cells/mL.

5.12.   Carefully add the 200 μL of the cell suspension dropwise in the seeding chamber.

5.13.   Allow the cells to settle at 37 °C in a CO_2 incubator for 2 h.

5.14.   Add microtissue fabrication medium surrounding the agarose mold to just cover the surface of the inner chamber.

5.15.   After 24 h, the cells self-assemble and compact significantly in the circular recesses. Replace with fresh medium every 2 days for maintenance.

6.   Fixation and permeabilization of cells and cardiac microtissues for immunostaining

6.1.   For each individual cell types, culture the cells separately on basement membrane matrix medium or gelatin coated chamber slides (approximately 25–30 x 10^4 cells/mL). Cardiac microtissues can be collected in 15 mL conical tube by gently flushing them out of the circular recesses.

397 6.2. Aspirate the medium and rinse the cells or microtissues with 1 mL PBS; thereafter, fix with
398 the fixation buffer containing 4.2% PFA for 20 min for the chamber slides and 1 h for microtissues
399 at room temperature.

401 6.3. Aspirate the PFA and add 1 mL of permeabilizing solution (0.25% Triton X-100 in PBS) for
402 5 to 7 min for chamber slides and 20 min for microtissues in 15 mL conical tube.

404 NOTE: From this step onwards, the samples can be gently rocked on a benchtop rocking platform.

406 6.4. Aspirate the permeabilizing solution and rinse once with 2 to 3 mL of PBS.

408 6.5. Incubate the cells with 500–1,000 µL of blocking solution (2% to 5% normal goat serum
409 or donkey serum) for at least 1 h for the chamber slides and 3 to 4 h for the microtissues.

411 6.6. Incubate the cells or cardiac microtissues with conjugated antibodies prepared in the
412 blocking solution sufficient to cover the sample. Incubate with anti-cardiac Troponin-T (cTnT2)
413 (1:50), anti-CD31 (1:75), and anti-DDR2/Vimentin (1:50) for 1 h for the chamber slides and
414 overnight at 4 °C for cardiac microtissues.

416 6.7. Wash the chamber slides three times with 500 µL 0.1% Tween-20 for 5 min between each
417 wash and a final wash with PBS.

419 6.8. For the cardiac microtissues, wash with 2 mL 0.1% Tween-20 five times with 20 min
420 duration between each wash. Perform a final wash step for an additional 20 min.

422 6.9. Incubate the cells or microtissues with 4',6-diamidino-2-phenylindole (DAPI) (1 µg/mL)
423 prior to confocal microscopy.

425 6.10. For cardiac microtissues, transfer carefully to a 35 mm glass bottom dish and add PBS to
426 submerge microtissues.

428 6.11. For 3D imaging, using a 20x or 40x oil immersion objective gain center focus of the
429 microtissue and adjust exposure parameters for each fluorophore.

431 6.12. For obtaining a Z-stack, set first and last coordinates in Live mode with a total imaging
432 depth of 100–200 µm with 5–10 µm slice interval.

434 **7. Digestion of cardiac microtissues and preparation of cells for flow cytometry**

436 7.1. To digest microtissues, gently flush the microtissues with Medium #1 out of the circular
437 recesses using a wide-bore 1 mL pipette tip into a 15 mL conical tube.

439 7.2. Allow the microtissues to settle and aspirate the medium carefully and rinse the cells or
440 microtissues with 1 mL PBS and add 200–300 µL of enzyme digestion buffer for 20 min at 37 °C.

441 At 10 min, mix the microtissues gently for 1 min and incubate again at 37 °C for the remainder of
442 time.

443

444 7.3.   After incubation, use a regular 1 mL pipette tip to mix the microtissues vigorously to
445 obtain a turbid cell suspension.

446

447 7.4.   Once the microtissues are sufficiently digested into single cells, immediately neutralize
448 the cell suspension with 5 mL of medium containing 5% FBS and strain the cell suspension
449 through a 40 μm cell strainer. Count the total number of cells and centrifuge the single cell
450 suspension at 300 x g for 5 min at 4 °C.

451

452 7.5.   Aspirate the supernatant and resuspend 1 x 10^5–1 x 10^6 cells in 100 μL annexin-binding
453 buffer with FITC Annexin V and 100 μg/mL propidium iodide (PI) or To-Pro3 dead cell exclusion
454 dye for 10 min on ice.

455

456 7.6.   After incubation, add 300 μL of the annexin binding buffer to the cell suspension and
457 transfer to a round bottom FACS tube for flow cytometry analysis. Use the correct lasers and
458 emission filters for the select fluorophores.

459

460 7.7.   For quantification of cell surface markers using fixed cells, perform the fixation and
461 permeabilization of the cell pellet as described in steps 6.2 and 6.3.

462

463 7.8.   After permeabilization, rinse the cell pellet and incubate the cells with respective
464 conjugated antibodies for 1 h. Wash the cell pellet in 4 mL FACS buffer (2% FBS in PBS) and
465 centrifuge at 300 x g for 3 min. Repeat the wash step twice.

466

467 7.9.   Resuspend the cells in 200–300 μL FACS buffer for flow cytometry analysis.

468

469 7.10.   Adjust the forward and side scatter properties with an unstained sample and consider
470 using an isotype control for each fluorophore to adjust the laser voltages. Collect a minimum of
471 20,000 events for data analysis.

472

473 **8.   Performing contraction analyses of spontaneously beating cardiac microtissues**

474

475 8.1.   Record videos of cardiac microtissues to capture at least three beats. Set the recording
476 resolution to at least 1280 x 720 pixels at frame rate >30 frames per second and save the video
477 in .AVI format.

478

479 8.2.   Run the MotionGUI script[11] in a MATLAB environment to launch the user interface.

480

481 8.3.   Find the .AVI file location in your folder to load the video. Then, enter the frame rate at
482 which the video was captured in the Input panel.

483

484 8.4.   In the advanced input panel, a pixel size may be specified based on the resolution and the

485   capture magnification.

486

487   8.5.   A suitable macroblock pixel size can be specified (default 16) and a detectable pixel
488   motion depending on the strength of microtissue contraction.

489

490   8.6.   After adjusting the parameters, click on **Get Motion Vectors** to begin the analysis.

491

492   8.7.   Select a region of interest with the **Choose AOI** radio button to exclude areas surrounding
493   the single microtissue in the circular recess.

494

495   8.8.   Use the function **Map Time Ave** to generate a mean contraction heatmap based on
496   motion detected on X and Y axes.

497

498   8.9.   For peak tracing data, use the function **Get Contraction Data** to automatically measure
499   the contraction and relaxation peaks.

500

501   8.10.   In the event of a low signal-to-noise ratio, apply a peak height and distance threshold to
502   correctly annotate the maximum contraction velocity (blue dot) and maximum relaxation velocity
503   (red triangle).

504

505   8.11.   After setting the correct thresholds, select **Analyze Peaks** to obtain the contraction and
506   relaxation values with beat rate and beat interval.

507

508   8.12.   Obtain measurements from a minimum of 25 individual microtissues for statistical
509   analyses.

510

511   **REPRESENTATIVE RESULTS:**

512

513   **Immunostaining and flow cytometry characterization of iPSC-derived CMs, ECs, and CFs**
514   To generate cardiac microtissues composed of iPSC-CMs, iPSC-ECs, and iPSC-CFs, all three cell
515   types are differentiated and characterized individually. *In vitro* differentiation of iPSCs to iPSC-
516   CMs has improved over the past several years. However, the yield and purity of iPSC-CMs differ
517   from line to line. The current protocol yields over 75% pure iPSC-CMs that spontaneously start
518   beating around day 9 (**Figure 1A**). Further purification steps from day 9 to day 14 can improve
519   iPSC-CM purity to over 80% as previously described[12]. Similarly, high-purity iPSC-ECs can be
520   generated using previously published protocols[13,14] that include the addition of several vascular
521   growth factors that polarize endothelial progenitors arising from the mesoderm around days 4–
522   5 (**Figure 1B**) to form phenotypically well-defined iPSC-ECs. iPSC-CFs are a highly heterogenous
523   population based on their location and are characterized based on their morphology and
524   expression of extracellular matrix proteins. Here, using published protocols[15-17] with
525   modifications, human iPSC-CFs are obtained from cardiac mesoderm progenitor cells (**Figure 1C**).

526

527   [*Figure 1*]

528

529 The purity of iPSC-CMs, iPSC-ECs, and iPSC-CFs were determined by immunostaining and flow
530 cytometry using Troponin-T (cTnT2), platelet endothelial cell adhesion molecule (PECAM1/CD31)
531 and vimentin (VIM), respectively (**Figure 2A**). Quantitative analysis showed a purified population
532 containing over 90% cTnT2 cells at day 20. iPSC-ECs obtained at day 12 after MACS sorting using
533 CD31 beads were identified with immunostaining against PECAM1/CD31 endothelial cell surface
534 marker. MACS sorting yielded highly pure endothelial cells as evidenced by over 95% CD31+ cells
535 at P0. However, it must be noted that the purity of endothelial cells decreased with higher
536 passage numbers due to de-differentiation. Similarly, at day 20, flow cytometry analyses revealed
537 that over 95% iPSC-CFs expressed the fibroblast marker VIM (**Figure 2B**).
538 [*Figure 2*]
539
540 **Fabrication of cardiac microtissue cultures and size analyses**
541 Single cell suspensions of iPSC-CMs, iPSC-ECs, and iPSC-CFs were mixed in 7:2:1 ratio and carefully
542 dispensed into the cell seeding chamber of the sterilized agarose replica mold (**Figure 3A,B**). The
543 cells uniformly settled inside the circular recesses in 2 h. Around day 3, the self-assembled cells
544 organize into uniform sized spontaneously beating cardiac microtissues (**Figure 3C**). Arrays of
545 different sized microtissues can be fabricated by tuning the final cell density (**Figure 3D,E**).
546 Cardiac microtissues fabricated with a final cell density of 1 x 10^6 cells/mL is ~300–350 μm in
547 diameter, 2 x 10^6 cells/mL is ~600 μm in diameter, and 4 x 10^6 cells/mL is over 800 μm n diameter.
548 Microtissue assembly was obtained with a cell density of 1 x 10^6 cells/mL, which is typically used
549 for experiments. These microtissue cultures can be maintained in culture for up to 6 weeks.
550 [*Figure 3*]
551
552 **Immunostaining and viability after enzymatic digestion**
553 Immunofluorescence staining of day 12 post-fabrication using antibodies against cTnT2 for iPSC-
554 CMs, CD31 for iPSC-ECs, and DDR2 for iPSC-CFs revealed a unique cell distribution in cardiac
555 microtissues. iPSC-CMs, the heaviest of all three cell types, occupied the center, whereas iPSC-
556 ECs were interspersed throughout the microtissues, and iPSC-CFs were observed to
557 predominantly occupy the periphery (**Figure 4A**). Short and rapid digestion of the microtissues
558 achieved using Dispase I and Liberase TL resulted in overall highly viable cell proportion (**Figure
559 4B, top panel**) with less than 5% apoptotic cells after 2 weeks in culture. This was followed by a
560 brief 1 h exposure of cardiac microtissues to a high concentration (5 μM) of Doxorubicin, a
561 chemotherapeutic drug that is known to induce dose-dependent cardiotoxicity (**Figure 4B,
562 bottom panel**).
563 [*Figure 4*]
564
565 **Computational contractility analysis**
566 Contractility analyses of individual cardiac microtissues can be performed with the help of a
567 MATLAB-based image analyses tool. Video recordings of spontaneously beating cardiac
568 microtissues were obtained at 30 fps for analysis. As described previously[11], the block-matching
569 method employs motion tracking algorithm to capture movement of a block of pixels for the total
570 frames acquired as a time series of motion vectors. The contractility of the microtissues and
571 movement of the vectors generate a pseudo heatmap that illustrates mean or average
572 contraction profile across the microtissue (**Figure 5A**). Contractile motion of the cardiac

573 microtissues generates positive peaks that are measured as contraction velocity (*blue circle*),
574 relaxation velocity (*red triangle*), and beat rate, the last of which is calculated as the time
575 between two contraction cycles (**Figure 5B**). Furthermore, the contractility of the cardiac
576 microtissues do not change significantly over 4 weeks in culture (**Figure 5C**).
577 [*Figure 5*]
578
579 **FIGURE AND TABLE LEGENDS:**
580
581 **Figure 1: Differentiation timeline.** Overall schematic of (**A**) iPSC-CM, (**B**) iPSC-EC, and (**C**) iPSC-CF
582 differentiation timeline with representative phase contrast images of cells after differentiation
583 and purification steps. Scale bar = 100 µm.
584
585 **Figure 2: Immunofluorescence and flow cytometry characterization.** (**A**) [Left to right panel]
586 iPSC-CMs at day 25 stained with cTnT2 (cyan), iPSC-ECs stained with PECAM1/CD31 (green), iPSC-
587 CFs stained with VIM (red), and nuclei stained with DAPI (blue). Scale bar = 50 µm. (**B**) [Left to
588 right panel] Flow cytometry quantification showed a high percent purity of iPSC-CMs (91.8%),
589 iPSC-ECs (98.1%), and iPSC-CFs (96.7%) following differentiation.
590
591 **Figure 3: Replica molding technique to generate multicellular cardiac microtissues.** (**A**) Replica
592 molded agarose microwell trays of (**B**) iPSC-CM, iPSC-EC, and iPSC-CF mixtures captured inside
593 the microwells for self-assembly. Scale bar 500 = µm. (**C**) Micrograph showing compaction of
594 cardiac microtissues on day 3. Scale bar = 500 µm. (**D**) Cardiac microtissue sizes formed show a
595 linear relationship with initial seeding densities, with higher cell densities resulting in larger
596 microtissues. (**E**) A representative figure showing the self-assembled cardiac microtissues in the
597 microwell array.
598
599 **Figure 4: Immunostaining of cardiac microtissues and assessment of cell viability.** (**A**) Confocal
600 z-stack images of human cardiac microtissue stained for iPSC-CMs (cTnT2), iPSC-ECs (CD31), iPSC-
601 CFs (DDR2), and nuclei stained with (DAPI). Scale bar = 200 µm. (**B**) Flow cytometry plots of
602 cardiac microtissues enzymatically digested into single cell suspension and stained with Annexin
603 V (apoptotic marker) and dead cell exclusion dye (To-Pro3). Digested single cell suspension
604 showed a high cell viability (91%) with <5% apoptotic cell population (top panel), compared to
605 single cell suspension treated with an apoptosis-inducing chemotherapeutic drug, Doxorubicin,
606 for 1 h at 5 µM concentration (bottom panel).
607
608 **Figure 5: Contraction analysis of cardiac microtissues.** (**A**) Phase contrast image and contraction
609 map of cardiac microtissues 1 week after fabrication. Scale bar = 200 µm. (**B**) Cardiac microtissues
610 show regular contraction and relaxation profiles and beat rates. Table shows representative
611 values of beat rate, maximum contraction, and relaxation velocities. (**C**) Long-term culture of
612 cardiac microtissues for up to 4 weeks does not significantly influence contractility parameters
613 (n = 20/group).
614
615 **DISCUSSION:**
616 To generate cardiac microtissues from pre-differentiated iPSC-CMs, iPSC-ECs, and iPSC-CFs, it is

617 essential to obtain a highly pure culture for better control of cell numbers after contact-inhibited
618 cell compaction within the cardiac microtissues. Recently, Giacomelli et. al.[18] have demonstrated
619 the fabrication of cardiac microtissues using iPSC-CMs, iPSC-ECs, and iPSC-CFs. Cardiac
620 microtissues generated using the described method consist of ~5,000 cells (70% iPSC-CMs, 15%
621 iPSC-ECs, and 15% iPSC-CFs). In this method, both cardiomyocytes and endothelial cells were co-
622 differentiated followed by separation of endothelial progenitors using CD34+ marker. The
623 current protocol described here consists of 12,000 cells (70% iPSC-CMs, 20% iPSC-ECs, and 10%
624 iPSC-CFs) per microtissue, which yields higher cell numbers per construct for downstream single
625 cell analyses. Furthermore, since all three cell types are differentiated separately there is limited
626 heterogeneity in cell populations that is unique to understanding cell-specific responses to
627 treatments.
628
629 For cardiomyocyte differentiation, we and others have previously demonstrated the derivation
630 of pure cardiomyocytes using chemically defined culture conditions[12,19,20]. Briefly, differentiation
631 begins with mesendoderm induction, followed by modulation of Wnt/β-catenin signaling that
632 promotes cardiac lineage specification. Further purification of the cardiomyocytes in a glucose-
633 deprived medium allows the elimination of non-cardiomyocytes. Here, it is important to note
634 that prolonged culture in purification medium can hamper the quality of cardiomyocytes. A
635 recently published protocol shows the proliferative capacity of early-stage cardiomyocytes can
636 be harnessed to obtain large number of cells. The expansion of human iPSC-CMs is induced with
637 reintroduction of CHIR, a potent mitogen during the early proliferative phase[21]. Although the
638 precise molecular mechanism is still unknown, this technique can significantly improve iPSC-CM
639 yield by ten-fold or hundred-fold. Furthermore, to improve the fidelity of iPSC-CMs for disease
640 modeling, they can be cultured in a maturation medium to enhance electrophysiological,
641 mechanical, and structural maturation[22]. A thorough overview of iPSC-CM maturation techniques
642 is reviewed elsewhere[23].
643
644 Vascular endothelial cells have been generated from pluripotent stem cells with different
645 purification variable efficiencies[13,24,25]. The current protocol provides high differentiation
646 efficiency and selection of phenotypically stable iPSC-ECs with MACS sorting[26]. The
647 differentiation methodology to generate functional cardiac fibroblasts follows modulation of the
648 Wnt pathway and fibroblast growth factor (FGF) signaling to generate iPSC-CFs[17] *In vivo* CFs
649 originate from epicardium, endocardium, and neural crest progenitors[16,27-29]. Here, the CF lineage
650 is generated from committed mesodermal cardiac progenitors without generating epicardial cells
651 as an intermediate. Overall, the protocols described here to generate iPSC-CMs, iPSC-ECs, and
652 iPSC-CFs take into account the ease of reproducibility and high purity based on phenotypic
653 characteristics. To obtain high quality microtissues, it is important to obtain >90% purity for each
654 individual cell type. Higher purity in the cellular phenotype will also ensure detection of changes
655 in cellular trajectory due to different treatments.
656
657 After successful derivation of all three cell types, the cells are carefully dispensed into the agarose
658 seeding chamber to allow settling of the cells in the circular recesses. Critical parameters include
659 achieving homogenous single cell suspension and preventing cell aggregates or clumps that may
660 cause variability in size distribution of the cardiac microtissues. From an overall structure

661 perspective, 3D constructs are often limited by diffusion of nutrients, and as the cell density
662 increases, the size and thickness of the constructs also increase linearly. Tissue engineered
663 constructs in the form of spherical structures have a uniform nutrient consumption rate due to
664 isotropic diffusivity and fixed distance from the core to the surface[30,31]. The final size of the
665 microtissue dictates the concentration gradient of nutrients and oxygen diffusion to the center.
666 In a static culture system, constructs over 350–400 µm may lead to a necrotic cell core when
667 cultured over longer periods of time. Hence, careful consideration should be given to seeding
668 density. A limitation of cardiac microtissue model is that it does not allow cardiomyocyte
669 alignment offered by methodologies that involve geometric confinement of single cells. Hence,
670 quantification of parameters such as sarcomere alignment or length remains limited due to
671 random multidimensional cellular assembly. Despite the limitation, the technique allows rapid
672 dose-dependent assessment of drug or small molecule toxicities on cardiovascular cells. In a
673 recent study, we employed 3D microtissues composed of iPSC-CMs to model secondary iron
674 overload-induced cardiomyopathy, and we observed a significant reduction in microtissue size
675 due to a high concentration of iron treatment[32].

677 With regard to immunostaining, unlike 2D cultures, longer permeabilization and primary
678 antibody incubation duration is necessary to allow diffusion of antibodies throughout the
679 microtissues. The incubation time for adequate antibody penetration may require further
680 optimization for microtissues larger than ~400 µm in diameter. Another important aspect is the
681 longer blocking step with serum proteins to reduce background fluorescence resulting from non-
682 specific binding. Typically, a blocking serum containing high IgG levels is preferred, such as goat
683 or donkey serum. In order to maintain structural integrity of the cardiac microtissues, we have
684 not probed for proteins involved in specific cell-cell interactions and their maintenance over the
685 culture period. For cellular phenotyping, the microtissues must be digested over a short period
686 of time to ensure high cell viability and preservation of target extracellular antigens. A
687 combination of enzymatic digestion and mechanical disruption with a wide-bore pipette tip
688 allows for an efficient and mild treatment of the microtissues during the digestion process. High
689 quality viable single cells obtained through this rapid digestion protocol can be used to elucidate
690 complex biological cell-cell interactions with the help of sc RNA-seq[33,34,35].

692 In addition to morphological and structural characterization, it is important to assess functional
693 properties of the cardiac microtissues to assess the efficacy, toxicity, and disease state of the
694 tissue assembly *in vitro*. Quantitative analysis of tissue contraction is a relevant parameter to
695 assess cardiac function. Several non-invasive video microscopy techniques combined with
696 motion tracking algorithms have enabled real-time monitoring with a robust measure of cardiac
697 tissue contraction linked to phenotypic characteristics. To quantify the changes in phenotype,
698 the cardiac microtissues can be maintained *in vitro* for up to 4 weeks without significant changes
699 in contractile parameters. Most software algorithms work on the principles of optical-flow and
700 vector mapping, which are superimposed over captured series of video frames[11,36,37]. The optical
701 flow analysis may lead to the detection of artifacts; hence, the user should avoid or minimize
702 inadvertent surrounding disturbances that could result in sample movement or vibrations
703 transmitted to the stage of the microscope. It must be noted that the contractility analyses may
704 not detect passive tension or loading effects due to suspended form of the microtissues, in

contrast to microtissues formed between flexible posts of pre-defined stiffness. However, in both cases, it is important to note that the contraction profiles of engineered cardiac muscle tissues do not achieve contraction forces generated at an organ level. The main advantages of image-based assays are that they are non-destructive and allow measurement of acute and chronic drug exposure without extensive calibration. These tools can be applied over a variety of 2D and 3D platforms to measure changes in cardiac contractility due to treatments or underlying genetic diseases, and to evaluate tissue maturation strategies. Future investigation of this microtissue model may involve combining electrophysiological measurements that will allow simultaneous recording of calcium- or voltage-sensitive dyes to obtain multiple independent recordings of each microtissue in an array in a high-throughput manner.

DISCLOSURES:
J.C.W. is a cofounder of Khloris Biosciences but has no competing interests, as the work presented here is completely independent. The other authors report no conflicts.

REFERENCES:

1.   Neofytou, E., O'Brien, C. G., Couture, L. A., Wu, J. C. Hurdles to clinical translation of human induced pluripotent stem cells. *Journal of Clinical Investigation.* **125** (7), 2551–2557 (2015).

2.   Lancaster, M. A., Knoblich, J. A. Organogenesis in a dish: Modeling development and disease using organoid technologies. *Science.* **345** (6194), 1247125–1247125 (2014).

3.   Liu, C., Oikonomopoulos, A., Sayed, N., Wu, J. C. Modeling human diseases with induced pluripotent stem cells: from 2D to 3D and beyond. *Development.* **145** (5), dev156166 (2018).

4.   Yin, X., Mead, B. E., Safaee, H., Langer, R., Karp, J. M., Levy, O. Engineering stem cell organoids. *Cell Stem Cell.* **18** (1), 25–38 (2016).

5.   Giacomelli, E. et al. Three-dimensional cardiac microtissues composed of cardiomyocytes and endothelial cells co-differentiated from human pluripotent stem cells. *Development* **144** (6), 1008–1017 (2017).

6.   Kurokawa, Y. K., George, S. C. Tissue engineering the cardiac microenvironment: Multicellular microphysiological systems for drug screening. *Advances in Drug Delivery Reviews.* **96**, 225–233 (2016).

7.   Cartledge, J. E. et al. Functional crosstalk between cardiac fibroblasts and adult cardiomyocytes by soluble mediators. *Cardiovascular Research.* **105** (3), 260–270 (2015).

8.   Ravenscroft, S. M., Pointon, A., Williams, A. W., Cross, M. J., Sidaway, J. E. Cardiac non-myocyte cells show enhanced pharmacological function suggestive of contractile maturity in stem cell derived cardiomyocyte microtissues. *Toxicology Science.* **152** (1), 99–112 (2016).

749   9.   Ieda, M. et al. Cardiac fibroblasts regulate myocardial proliferation through beta1 integrin
750   signaling. *Developmental Cell.* **16** (2), 233–244 (2009).
751   10.   Brutsaert, D. L. Cardiac endothelial-myocardial signaling: its role in cardiac growth,
752   contractile performance, and rhythmicity. *Physiological Reviews.* **83** (1), 59–115 (2003).
753   11.   Huebsch, N. et al. Automated video-based analysis of contractility and calcium flux in
754   human-induced pluripotent stem cell-derived cardiomyocytes cultured over different spatial
755   scales. *Tissue Engineering Part C Methods.* **21** (5), 467–479 (2015).
756   12.   Burridge, P. W. et al. Chemically defined generation of human cardiomyocytes. *Nature
757   Methods.* **11** (8), 855–860 (2014).
758   13.   Gu, M. *et al.* Pravastatin reverses obesity-induced dysfunction of induced pluripotent stem
759   cell-derived endothelial cells via a nitric oxide-dependent mechanism. *European Heart Journal.*
760   **36** (13), 806–816 (2015).
761   14.   Williams, I. M., Wu, J. C. Generation of endothelial cells from human pluripotent stem cells.
762   *Arteriosclerosis, Thrombosis and Vascular Biology.* **39** (7), 1317–1329 (2019).
763   15.   Zhang, H., Shen, M., Wu, J. C. Generation of quiescent cardiac fibroblasts derived from
764   human induced pluripotent stem cells. *Methods in Molecular Biology.* Springer, New York. 1-7
765   (2020).
766   16.   Zhang, H. et al. Generation of quiescent cardiac fibroblasts from human induced
767   pluripotent stem cells for in vitro modeling of cardiac fibrosis. *Circulation Research.* **125** (5), 552–
768   566 (2019).
769   17.   Zhang, J. et al. Functional cardiac fibroblasts derived from human pluripotent stem cells
770   via second heart field progenitors. *Nature Communications.* **10** (1), 2238–2315 (2019).
771   18.   Giacomelli, E. et al. Human-iPSC-derived cardiac stromal cells enhance maturation in 3d
772   cardiac microtissues and reveal non-cardiomyocyte contributions to heart disease. *Cell Stem Cell.*
773   **26** (6), 862–879.e11 (2020).
774   19.   Burridge, P. W., Holmström, A., Wu, J. C. Chemically defined culture and cardiomyocyte
775   differentiation of human pluripotent stem cells. *Current Protocols in Human Genetics* **87** (1),
776   21.3.1–21.3.15 (2015).
777   20.   Lian, X. et al. Directed cardiomyocyte differentiation from human pluripotent stem cells
778   by modulating Wnt/β-catenin signaling under fully defined conditions. *Nature Protocols.* **8** (1),
779   162–175 (2013).
780   21.   Buikema, J. W. et al. Wnt activation and reduced cell-cell contact synergistically induce
781   massive expansion of functional human iPSC-derived cardiomyocytes. *Cell Stem Cell.* **27** (1), 50–
782   63.e5 (2020).
783   22.   Feyen, D. A. M. et al. Metabolic maturation media improve physiological function of
784   human iPSC-derived cardiomyocytes. *Cell Reports.* **32** (3), 107925 (2020).
785   23.   Karbassi, E. et al. Cardiomyocyte maturation: Advances in knowledge and implications for
786   regenerative medicine. *Nature Reviews Cardiology.* **17** (6), 341–359 (2020).
787   24.   Li, Z., Hu, S., Ghosh, Z., Han, Z., Wu, J. C. Functional characterization and expression
788   profiling of human induced pluripotent stem cell- and embryonic stem cell-derived endothelial
789   cells. *Stem Cells Development.* **20** (10), 1701–1710 (2011).
790   25.   Lian, X. et al. Efficient differentiation of human pluripotent stem cells to endothelial
791   progenitors via small-molecule activation of WNT signaling. *Stem Cell Report.* **3** (5), 804–816
792   (2014).

793 26. Gu, M. Efficient differentiation of human pluripotent stem cells to endothelial cells. *Current Protocols in Human Genetics.* **98** (1), e64 (2018).

795 27. Acharya, A. *et al.* The bHLH transcription factor Tcf21 is required for lineage-specific EMT of cardiac fibroblast progenitors. *Development.* **139** (12), 2139–2149 (2012).

797 28. Wessels, A. et al. Epicardially derived fibroblasts preferentially contribute to the parietal leaflets of the atrioventricular valves in the murine heart. *Development Biology.* **366** (2), 111–124 (2012).

800 29. Ali, S. R. et al. Developmental heterogeneity of cardiac fibroblasts does not predict pathological proliferation and activation. *Circulation Research.* **115** (7), 625–635 (2014).

802 30. McMurtrey, R. J. Analytic and numerical models of oxygen and nutrient diffusion, metabolism dynamics, and architecture optimization in three-dimensional tissue constructs with applications and insights in cerebral organoids. *Tissue Engineering Part C Methods* (3), 221–249 (2015).

806 31. Thomas, D., O'Brien, T., Pandit, A. Toward customized extracellular niche engineering: progress in cell-entrapment technologies. *Advanced Materials.* **30** (1), 1703948 (2018).

808 32. Rhee, J.-W. *et al.* Modeling secondary iron overload cardiomyopathy with human induced pluripotent stem cell-derived cardiomyocytes. *Cell Reports.* **32** (2), 107886 (2020).

810 33. Paik, D. T., Cho, S., Tian, L., Chang, H. Y., Wu, J. C. Single-cell RNA sequencing in cardiovascular development, disease, and medicine. *Nature Reviews Cardiology.* **17** (8), 457–473 (2020).

813 34. Nguyen, Q. H., Pervolarakis, N., Nee, K., Kessenbrock, K. Experimental considerations for single-cell RNA sequencing approaches. *Frontiers in Cell and Developmental Biology.* **6**, 108 (2018).

816 35. Lau, E., Paik, D. T., Wu, J. C. Systems-wide approaches in induced pluripotent stem cell models. *Annual Reviews in Pathology.* **14** (1), 395–419 (2019).

818 36. Maddah, M. et al. A non-invasive platform for functional characterization of stem-cell-derived cardiomyocytes with applications in cardiotoxicity testing. *Stem Cell Report.* **4** (4), 621–631(2015).

821 37. Sala, L. et al. Musclemotion: A versatile open software tool to quantify cardiomyocyte and cardiac muscle contraction in vitro and in vivo. *Circulation Research.* **122** (3), e5–e16 (2018).
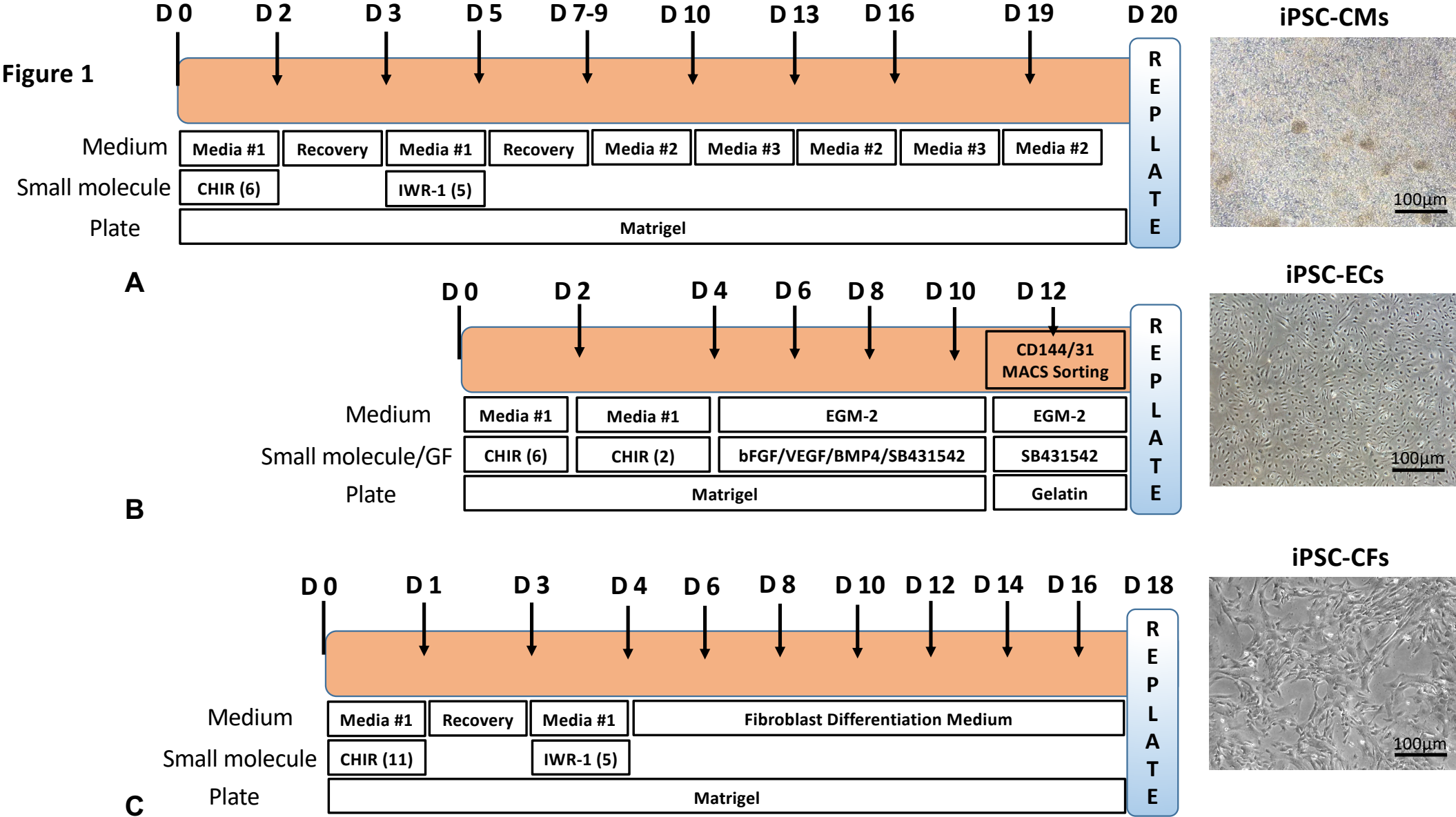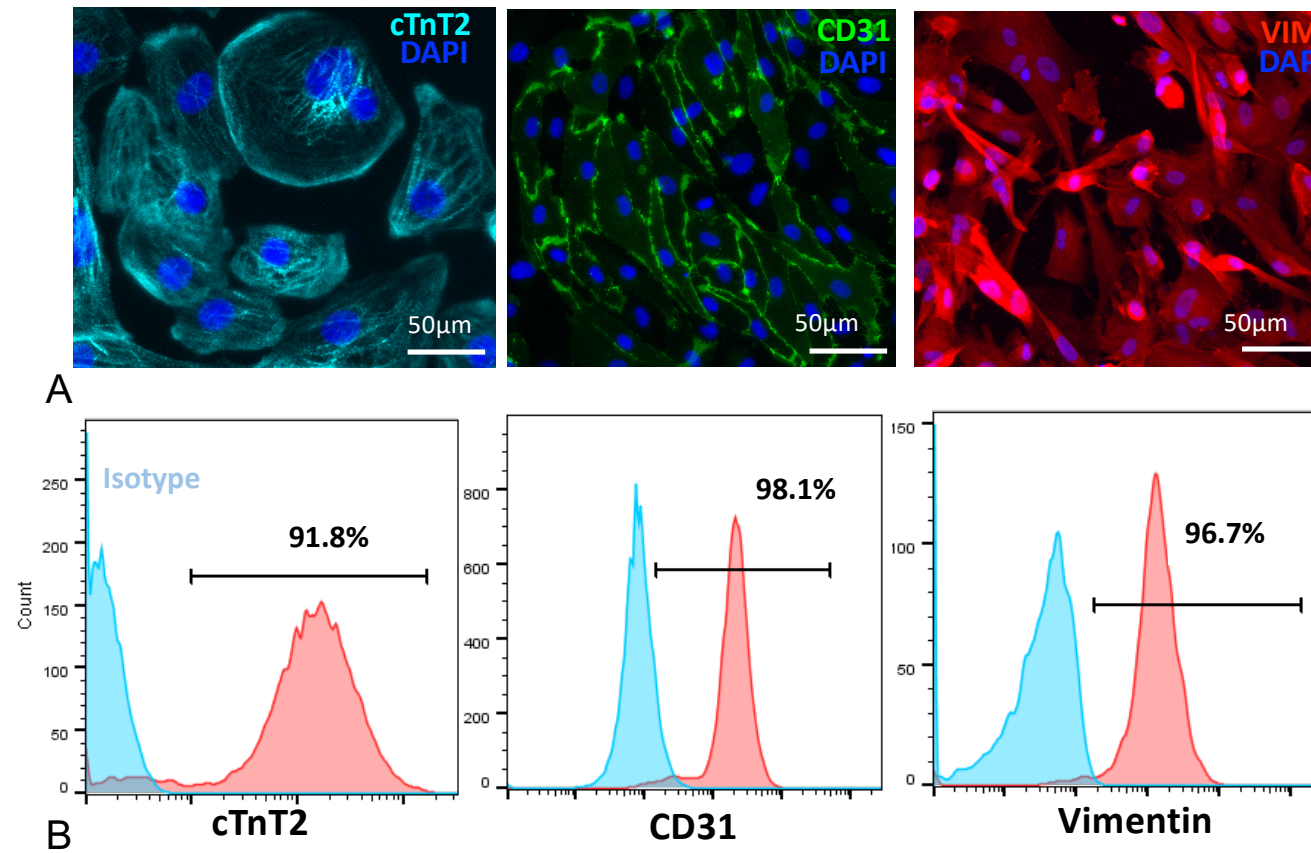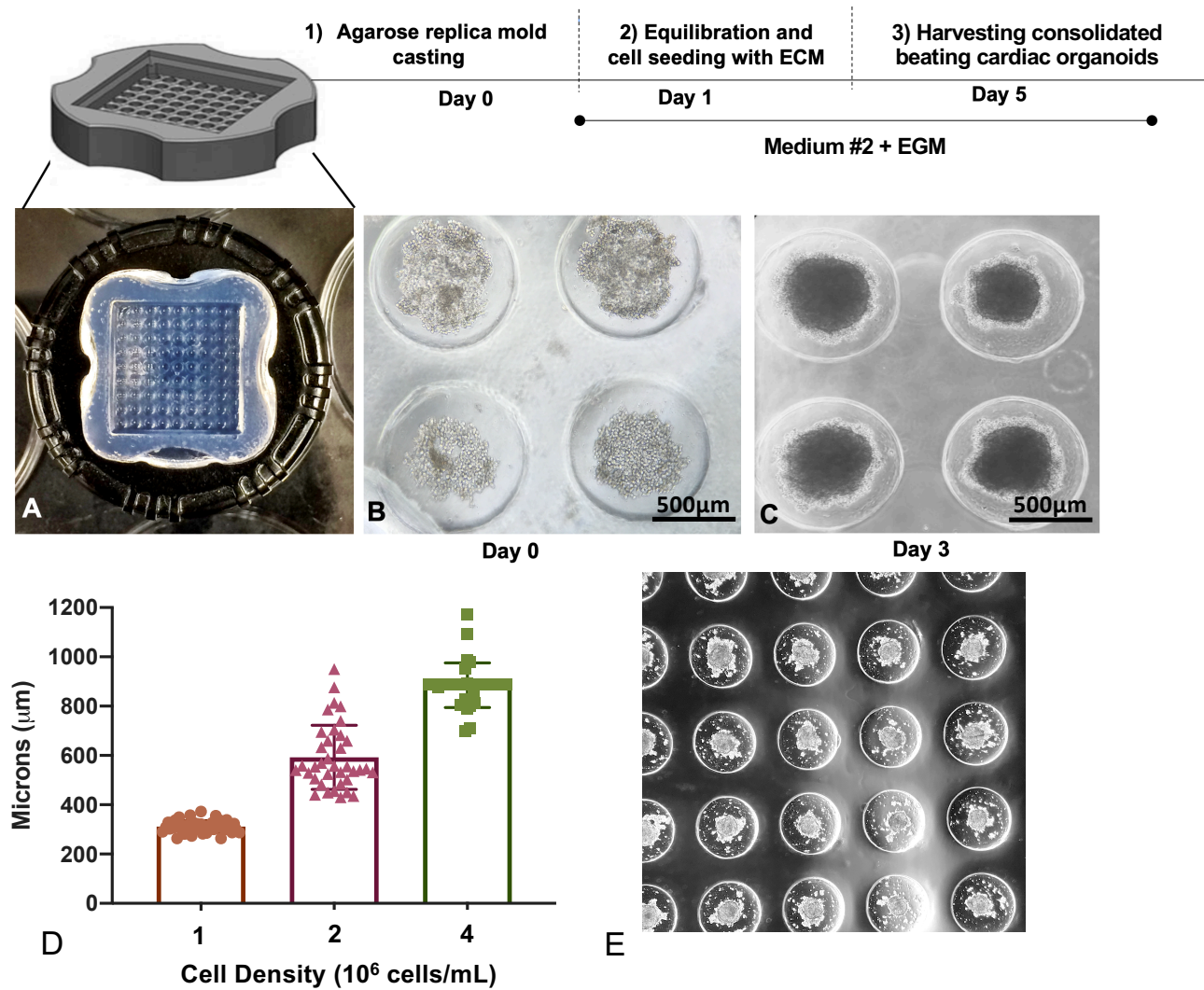
823

Figure 1

A

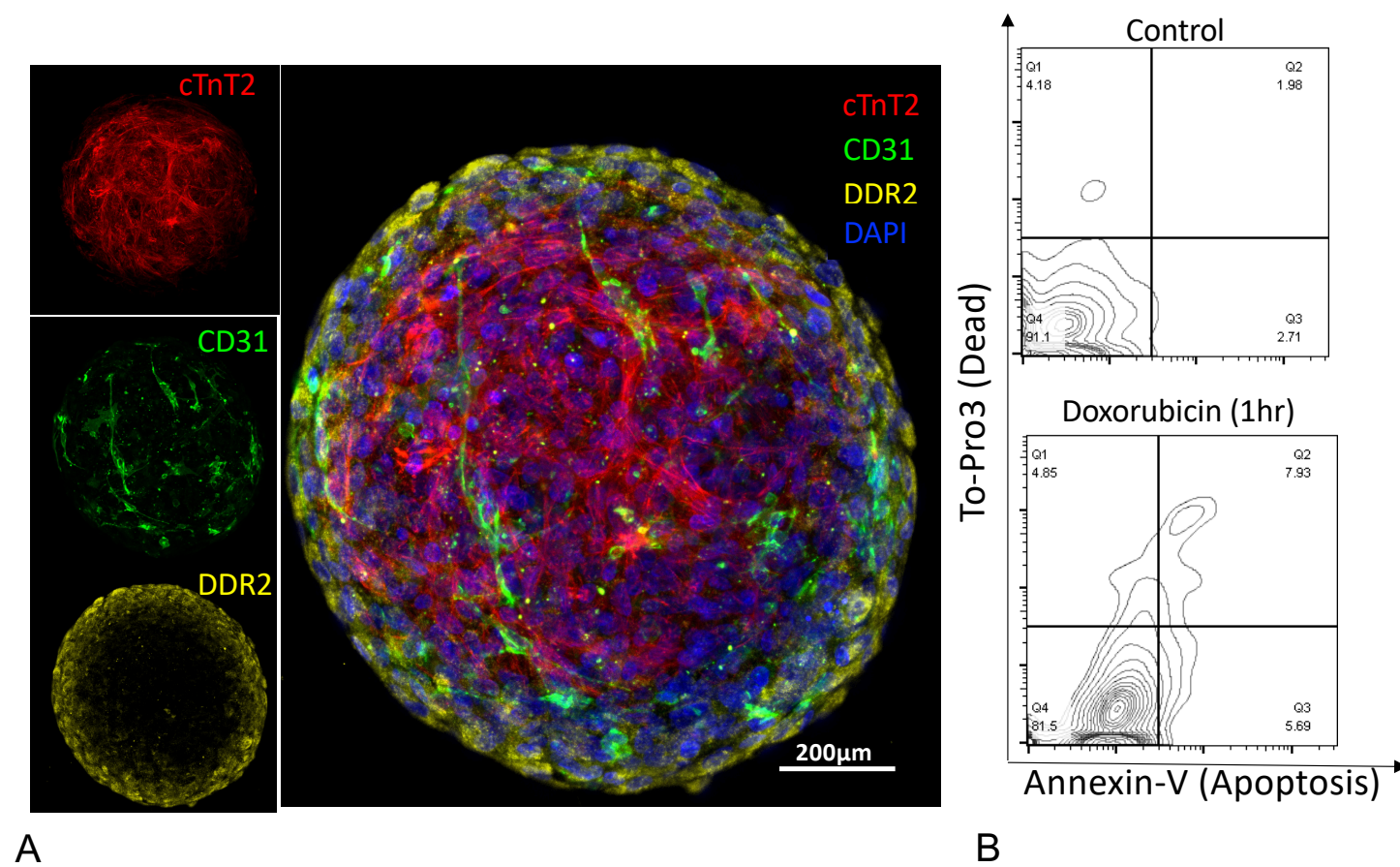**iPSC-CMs**

Timeline: D 0, D 2, D 3, D 5, D 7-9, D 10, D 13, D 16, D 19, D 20 → REPLATE

Medium: Media #1 | Recovery | Media #1 | Recovery | Media #2 | Media #3 | Media #2 | Media #3 | Media #2

Small molecule: CHIR (6) | IWR-1 (5)

Plate: Matrigel

Scale bar: 100μm

B

iPSC-ECs

Timeline: D 0, D 2, D 4, D 6, D 8, D 10, D 12 → CD144/31 MACS Sorting → REPLATE

Medium: Media #1 | Media #1 | EGM-2 | EGM-2

Small molecule/GF: CHIR (6) | CHIR (2) | bFGF/VEGF/BMP4/SB431542 | SB431542

Plate: Matrigel | Gelatin

Scale bar: 100μm

C

iPSC-CFs

Timeline: D 0, D 1, D 3, D 4, D 6, D 8, D 10, D 12, D 14, D 16, D 18 → REPLATE

Medium: Media #1 | Recovery | Media #1 | Fibroblast Differentiation Medium

Small molecule: CHIR (11) | IWR-1 (5)

Plate: Matrigel

Scale bar: 100μm

Figure 2

Figure 2

Figure 3

Figure 3

1) Agarose replica mold casting — Day 0

2) Equilibration and cell seeding with ECM — Day 1

3) Harvesting consolidated beating cardiac organoids — Day 5

Medium #2 + EGM

Figure 4

Figure 4

A

B

Figure 5

Figure 5

Beat Rate (bpm)	Avg Max Contraction Velocity (µm/sec)	Avg Max Relaxation Velocity (µm/sec)
30 ± 2	67.13 ± 4	33.17 ± 3.5

Name of Material/ Equipment	Company	Catalog Number	Comments/Description
12-well plates	Fisher Scientific	08-772-29	
3D micro-molds	Microtissues	12-81 format	
6-well plates	Fisher Scientific	08-772-1B	
AutoMACS Rinsing Solution	Thermo Fisher Scientific	NC9104697	
B27 Supplement minus Insulin	Life Technologies	A1895601	
B27 Supplement plus Insulin	Life Technologies	17504-044	
BD Cytofix	BD Bioscienc	554655	
BD Matrigel, hESC-qualified matrix	BD Bioscienc	354277	
Cardiac Troponin T Antibody	Miltenyi	130-120-403	
CD144 (VE-Cadherin) MicroBeads	Miltenyi	130-097-857	
CD31 Antibody	Miltenyi	130-110-670	
CD31 Microbeads	Miltenyi	130-091-935	
CHIR-99021	Selleckchem	S2924	
DDR2	Santa Cruz Biotechnology	sc-81707	

Dead Cell Apoptosis Kit with Annexin V FITC and PI	Thermo Fisher Scientific	V13242
Dispase I	Millipore Sigma	4942086001
DMEM, high glucose (4.5g/L) no glutamine media		11960044
DMEM/F-12 basal medium	Gibco	11320033
Dulbecco's phosphate buffered saline (DPBS), no calcium, no magnesium	Life Technologies	14190-136
EGM2 BulletKit	Lonza	CC-3124
Fetal bovine serum	Life Technologies	10437
FibroLife Serum-Free Fibroblast LifeFactors Kit	LifeLIne Cell Technology	LS-1010
Glucose free RPMI media	Life Technologies	11879-020
Goat serum	Life Technologies	16210-064
Human FGF-basic	Thermo Fisher Scientific	13256029
Human VEGF-165	PeproTech	100-20
IWR-1-endo	Selleckchem	S7086

	Millipore	
Liberase TL	Sigma	5401020001
LS Sorting Columns	Miltenyi	130-042-401
MACS BSA Stock solution	Miltenyi	130-091-376
MACS Rinsing Buffer	Miltenyi	130-091-222
MidiMACS Separator	Miltenyi	130-042-302
RPMI media	Life Technologies	11835055
SB431542	Selleckchem	S1067
TO-PRO 3	Thermo Fisher Scientific	R37170
Triton X-100	Millipore Sigma	X100-100ML
TrypLE Select 10X	Thermo Fisher Scientific	red
Vimentin Alexa Fluor® 488-conjugated Antibody	R&D Systems	IC2105G

JoVE submission JoVE61879

"**Fabrication of 3D Cardiac Microtissue Arrays Using Human iPSC-Derived Cardiomyocytes, Cardiac Fibroblasts, and Endothelial Cells**"

Response to Editorial and Reviewer comments:
We are grateful to the Editor and the Reviewers for reviewing our work and providing insightful feedback. We are thankful to the **4 reviewers** who have now endorsed our protocol. We have revised our manuscript based on comments from the additional **3 reviewers** that were newly assigned. All changes to the manuscript are highlighted in blue for tracking.

Editorial Comments:
1. Please address specific comments marked in the manuscript.
We have now addressed all specific comments marked in the manuscript.

2. Please address all reviewers' comments.
We have now addressed all 7 reviewers comments.

3. Please ensure that the highlight is no less than 1 page and no more than 3 pages including headings and spacings. Notes cannot be filmed.
We have now highlighted additional portions of the protocol for filming.

Reviewer #5:
Minor Concerns:
1: In figure 4, cardiac microtissues were immunostained with different markers to show cell composition. How many days of cardiac microtissues after fabrication did you use here? Could you provide a 3-D view of this z-stack images? Does the time of culture after fabrication affect the composition of this 3D cardiac sphere?

We thank the reviewer for the comment. The cardiac microtissues in this protocol have been cultured for 10 days. We have now included a 3D view of the z-stack images in the response to reviewers. Figure 1 shows a 3D reconstruction of the Z-stack images taken across ~80 µm from top to bottom with and interval of 8 µm. We are currently in the process of enumerating the cell composition as a function of time and

Figure 1: (left) A Z-stack 3D visualization of cardiac microtissue; (right) A pseudocolor field of depth view of cardiac microtissue with a step-size interval of 8µm from top to bottom.

treatment, and thus we have not included this in the protocol. For the scope of this protocol, we have detailed an optimized digestion of the microtissues that will enable users to quantify the cell proportions systematically using flow cytometry.
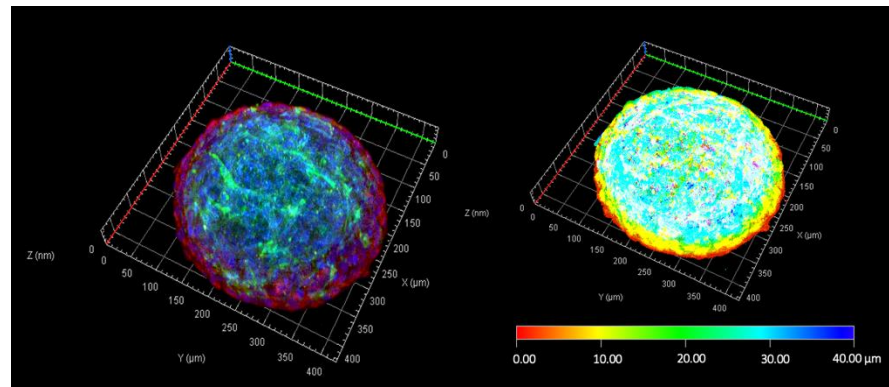
2: Figure 5 shows the contraction map of cardiac microtissues 1 week after fabrication. How long could cardiac microtissues show regular contraction and relaxation? Is there any relationship between the contraction capability and the time of culture after fabrication?

We thank the reviewer for their question. The cardiac microtissues can be maintained

Figure 2: (A) Maximum Contraction and (B) Relaxation velocities of untreated cardiac microtissues remain comparable between week 1 and week 4 in culture; n=20/group.

for up to 1 month in culture. We have now included week 1 and week 4 contractility data (n=20) as **Figure 5C** in the protocol (Figure 2 in Response to Reviewers) to demonstrate that the contraction and relaxation velocity remain comparable for up to 4 weeks in culture.
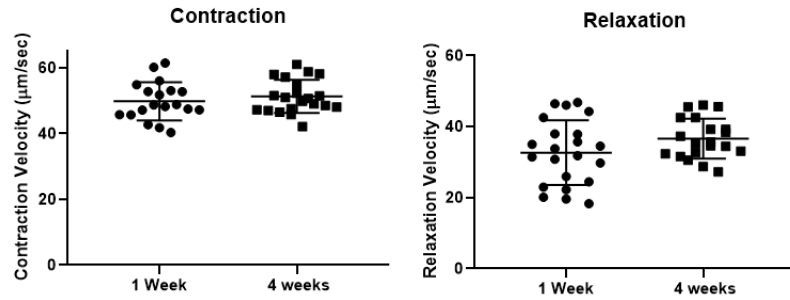
3: This manuscript described that cell-cell signaling arising from supporting cell types such as ECs and CFs was faithful recapitulated in this 3D self-assembled cardiac microtissue. I think it is better to show the cell junctions between CMs and CMs or CMs and CFs by immunostaining in figure 4 to provide a strong evidence.

We thank the reviewer for this comment and suggestion. For clarification, in the introduction of the current protocol, we have described the utility of the model in dissecting effects due to cell-cell interactions. In this protocol, we do not claim the establishment of specific cell-cell junctions. To clarify this, we have now added the following line in the discussion: Lines 678-680: "*In order to maintain structural integrity of the cardiac microtissues, we have not probed for proteins involved in specific cell-cell interactions and their maintenance over the culture period.*"

Reviewer #6:
Minor Concerns:
Are the cardiac fibroblasts activated or non-activated in this culture method? Please show experimental evidence, e.g., by alpha smooth muscle actin staining.

We thank the reviewer for this comment. The method described in the protocol utilizes cardiac fibroblasts generated from human iPSCs that are quiescent and express all cardiac fibroblasts markers (COL-I, DDR2, VIM, and POSTN), as we have demonstrated in recent publications (**Reference 13 and 14**). In this protocol, we aim to demonstrate the feasibility of generating cardiac microtissues with phenotypically well characterized cells. However, we acknowledge that these cell types could undergo several fates dependent on the perturbation. Therefore, we recommend the users to run appropriate controls to validate cell fate related changes such as fibroblast activation. To clarify this, we have now included the following line in the discussion: *"Higher purity in the cellular phenotype will also ensure detection of changes in cellular trajectory due to different treatments."*

Figure 2: FACS panels - the middle panel did not show in one version of the pdf. Best to check at proof stage.

Thank you for the comment. In the newly compiled figures, we can confirm the middle panel now appears correctly, and will be mindful of this comment as we review any final proofs.

Figure 3: Panel D - add 'cell density' to x-axis

We thank the reviewer for this correction. "Cell Density" is now added to the x-axis.

Reviewer #7:
Major Concerns:

In Figure 5, the velocity vector profiles measured from the cluster appear to have three peaks. It is unclear how the software used has parametrized these peaks - are the first two considered as contraction and the third one as relaxation? I assume this to be due to the temporal difference of contraction onset and propagation in different parts of the cluster. Thus, the selected approach of measuring contraction for the whole cluster without directional information does not appear to characterize the contraction mechanics in a way that is comparable between different clusters.

We thank the reviewer for this comment. It is correct that the first and second peak-split is the contraction and the third one is relaxation. Once the cardiac microtissue is fully formed, they do not beat as separate clusters within a single microtissue. However, as the reviewer alluded to, occasional acentric contraction does result in split peak. During analyses, this does not affect the annotation of the contraction and relaxation peaks as the "Min. Peak Distance" is pre-defined. To avoid further confusion and for clarity, the contraction profile and associated microtissue micrographs are now replaced with a more representative example.

Minor Concerns:

Discussion, line 598: the percentage should be 70% iPSC-CMs instead of 75% as per the reported Giacomelli et al. protocol.

We thank the reviewer for pointing out this error. We have now changed the percentage from 75 to 70 on line 613 of the revised protocol.

Discussion, lines 668-671. The authors are right in pointing out that contractility analysis does not detect effects of passive tension or loading. However, I would point out that micropillars and flexible posts also influence the contraction of the cluster, as the cells adhere to the micropost tips - an environment is not typical to the cells in vivo.

We thank the reviewer for this suggestion. We have now included the discussion as follows:

Line 692-696 *"It must be noted that the contractility analyses may not detect passive tension or loading effects due to suspended form of the microtissues, in contrast to microtissues formed between flexible posts of pre-defined stiffness. However, in both cases, it is important to note that the contraction profiles of engineered cardiac muscle tissues do not achieve contraction forces generated at an organ-level."*

Figure 1: The text, text boxes and images are poorly aligned, and the font size is inconsistent. Please revise.

We thank the reviewer for this comment. We have now corrected the formatting inconsistencies in Figure 1.

Figure 2: Although not key to reading the sorting graph, the axes of the three plots should have either consistent axis ticks or values.

We thank the reviewer for this comment and apologize for the inconsistency. Cell numbers gated for each cell type is different. Therefore, for consistency we have now replaced the scatter plots denoting the total cell count on the Y-axis.

Figure 4: Please make sure the DAPI text box does not cover the text above or the immunostaining image, and that the scale bar is not coloured.

Thank you for the comment. We now confirm the DAPI label and the scale bar appear correctly prior to PDF conversion. This will be further verified at the proof stage.

Figure 5 caption: Please be more specific in indicating the measured distribution of values of the contraction heatmap. At what point during the contraction is the velocity distribution measured? Related to protocol 8 stage 8.

We thank the reviewer for this comment. We would like to clarify that the contraction heatmap is a mean of the motion detected on X and Y axes. We have now revised protocol 8 and stage 8 as follows:

"The function "Map Time Ave." can be used to generate a mean contraction heatmap based on motion detected on X and Y axes."

Figure 5B: Make sure to use consistent terms to indicate that the values in table are velocities and use the same abbreviation for second as in 5A.

We thank the reviewer for bringing this to our attention. We have now used consistent terms in Figure 5 to describe the velocity measurements.